

# A multiwavelength study of the ISM and star formation in early-type galaxies

TAKUMA KOKUSHO,<sup>1</sup> HIDEHIRO KANEDA,<sup>1</sup> MARTIN BUREAU,<sup>2</sup> TOYOAKI SUZUKI,<sup>1</sup> KATSUHIRO MURATA,<sup>3</sup>  
AKINO KONDO,<sup>1</sup> AND MITSUYOSHI YAMAGISHI<sup>4</sup>

<sup>1</sup>Graduate School of Science, Nagoya University, Chikusa-ku, Nagoya 464-8602, Japan

<sup>2</sup>Sub-department of Astrophysics, Department of Physics, University of Oxford, Denys Wilkinson Building, Keble Road, Oxford OX1 3RH, UK

<sup>3</sup>Department of Physics, School of Science, Tokyo Institute of Technology, 2-12-1 Ohokayama, Meguro, Tokyo, 152-8551, Japan

<sup>4</sup>Institute of Space and Astronautical Science, Japan Aerospace Exploration Agency, 3-1-1 Yoshinodai, Chuo-ku, Sagami-hara, Kanagawa 252-5210, Japan

## ABSTRACT

We perform a systematic study of the interstellar medium (ISM) and star formation for a large sample of local early-type galaxies (ETGs) based on the *AKARI* all-sky maps. Our sample galaxies are the 260 ETGs from the ATLAS<sup>3D</sup> survey, for which cold gas measurements (CO and H I) are available. Combining the *AKARI* measurements with the 2MASS and *WISE* archival data, we modeled spectral energy distributions of the ETGs to derive the total dust and polycyclic aromatic hydrocarbon luminosities, and thus total dust masses and star formation rates (SFRs). We find that the dust-to-stellar mass ratios and the current SFRs of the ETGs are smaller than those of late-type galaxies (LTGs), showing that local ETGs are quiescent galaxies. We also find that the current star formation efficiencies of the ETGs are similar to those of LTGs. Our result suggests that low SFRs of local ETGs are likely caused by their smaller amounts of the cold ISM rather than a suppression of star formation.

**Keywords:** galaxies: elliptical and lenticular, cD - galaxies: ISM - galaxies: photometry - dust, extinction - infrared: galaxies - galaxies: star formation

## 1. INTRODUCTION

Early-type galaxies (ETGs), composed of lenticular and elliptical galaxies, show optical red colors, suggesting that ETGs are dominated by old stars at the late stage of galaxy evolution (e.g., [Thomas et al. 2010](#)). The galaxy evolution diagram predicts that late-type galaxies (LTGs) evolve into ETGs through galaxy mergers, exhausting the cold interstellar medium (ISM) through merger-induced star formation and/or active galactic nuclei (AGN) activities (e.g., [Hopkins et al. 2008](#)). Such merger-induced processes are thought to suppress star formation in ETGs by heating and perhaps expelling the cold ISM from a galaxy (e.g., [Schawinski et al. 2006](#)). Nevertheless recent observations detect cold dust and gas from many ETGs (e.g., [Temi et al. 2003](#); [Smith et al. 2012](#); [Amblard et al. 2014](#)), indicating that ETGs still form stars contrary to the above expectations. Hence it is crucial to investigate the ISM and star formation properties of ETGs to understand galaxy evolution.

In the present study, we perform a systematic study of the ISM and star formation for a large sample of local ETGs using the *AKARI* all-sky maps, estimating the star formation rates (SFRs) and dust masses of the ETGs. Combining the *AKARI* measurement with those of cold gas (CO and H I), we discuss the ISM and star formation properties of the ETGs.

## 2. SAMPLE AND DATA

Our sample is the 260 local ETGs from the ATLAS<sup>3D</sup> survey ([Cappellari et al. 2011](#)). Within the framework of this project, the sample ETGs were investigated by various observations, such as optical integral field spectroscopy, CO, and H I observations ([de Zeeuw et al. 2002](#); [Young et al. 2011](#); [Serra et al. 2012](#)). Although such a diverse range of observations was performed for the ATLAS<sup>3D</sup> ETGs so far, their infrared (IR) dust emission was not studied in detail. Accordingly, with the *AKARI* mid- and far-IR all-sky maps ([Doi et al. 2015](#); [Ishihara et al., in prep.](#)), we systematically measure IR flux densities of the ETGs at the 9, 18, 65, 90, and 140  $\mu\text{m}$  bands through aperture photometry with a circular aperture, whose radius is determined by optical extents of each galaxy and the point spread functions of the *AKARI* instruments ([Kokusho](#)

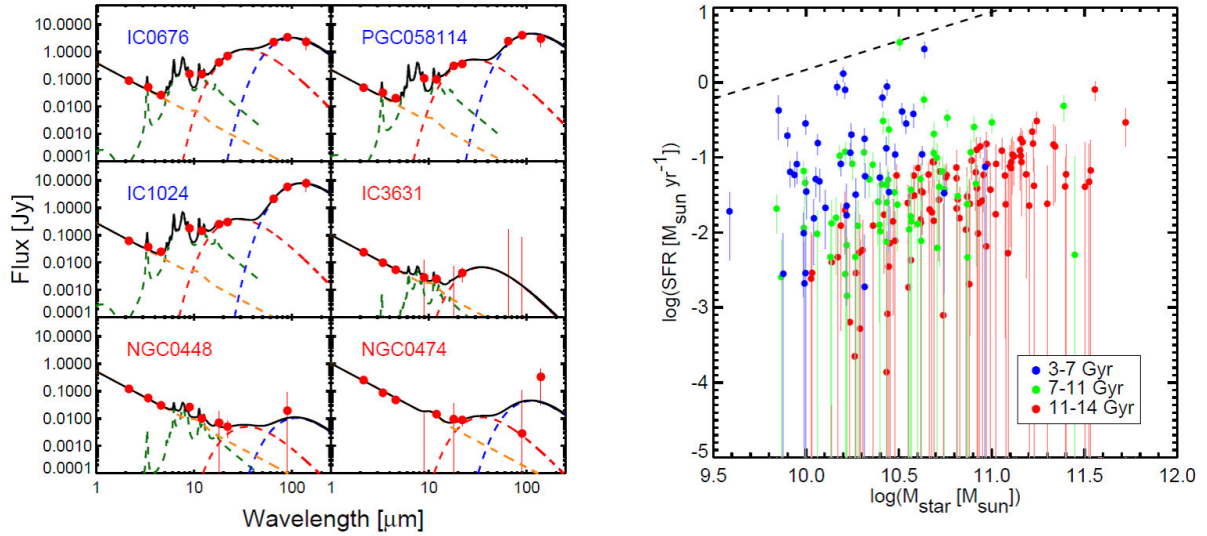


**Figure 1.** Left: examples of the spectral energy distributions of the sample galaxies. The best-fit stellar, PAH, warm, and cold dust models are shown in orange, green, red, and blue, respectively. The names of CO-detected and non-CO-detected galaxies are shown in blue and red, respectively. Right: star formation rates of the sample galaxies, plotted against their stellar masses. The galaxies with the stellar population age of 3–7, 7–11, and 11–14 Gyr are shown in blue, green, and red, respectively. Black dotted line shows the relation of late-type galaxies (Elbaz et al. 2007). Adapted from Kokusho et al. (2017).

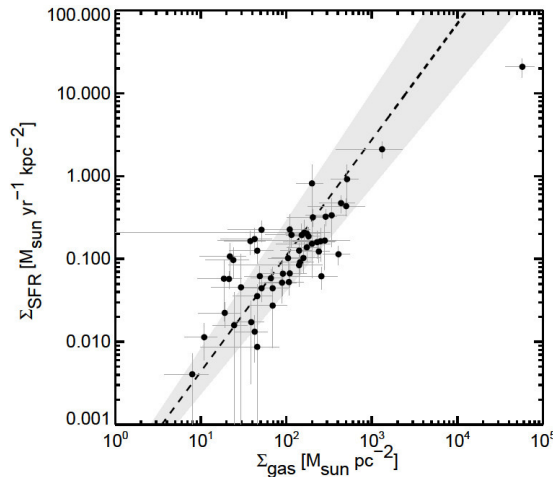


**Figure 2.** Correlation between the surface densities of star formation rates and gas masses for CO-detected galaxies. Black dotted line and gray shaded region show the relation of late-type galaxies and its intrinsic scatter, respectively (Kennicutt 1998). Adapted from Kokusho et al. (2017).

et al. 2017). We robustly detect far-IR emission from 45% of the sample ETGs (i.e. signal-to-noise ratio  $S/N > 3$  in at least one *AKARI* far-IR band), showing that cold dust is prevalent in ETGs.

Combing our *AKARI* measurements with the 2MASS and *WISE* archival data, we created spectral energy distributions (SEDs) of the sample ETGs. We then performed SED fits for each galaxy with a model composed of stellar, polycyclic aromatic hydrocarbon (PAH), and two-temperature dust emissions. We applied a power-law model for the stellar continuum and the Draine & Li (2007) model for the PAH emission, where a size distribution and ionized fraction of PAHs are fixed to those typical of LTGs. For the warm and cold dust emission, we used a modified blackbody model with emissivity power-law index of 2. The left panel of Figure 1 shows examples of the SEDs of the sample ETGs and their best-fit model, where the names of CO-detected and non-CO-detected ETGs are shown in blue and red, respectively (Young et al. 2011). The figure represents that CO-detected ETGs tend to show relatively strong PAH and dust emissions. Because PAHs can be a good star formation tracer (e.g., Shipley et al. 2016), this result indicates that molecular gas in ETGs is likely to fuel their current star formation.

### 3. RESULTS

The right panel of Figure 1 shows the current SFRs of the sample ETGs estimated from the best-fit PAH model, plotted against their stellar masses derived in the ATLAS<sup>3D</sup> survey (Cappellari et al. 2013). To derive the SFRs, we calculated

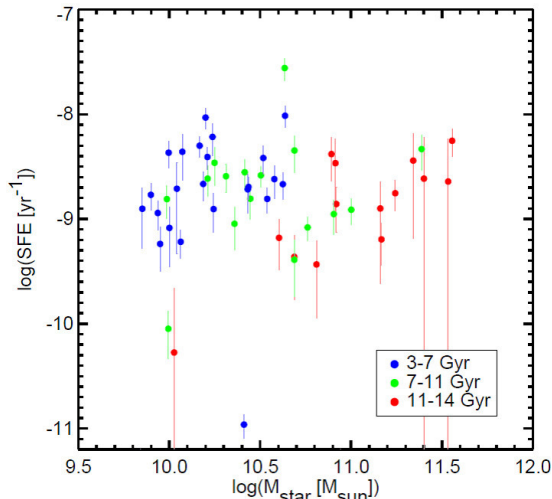


**Figure 3.** Star formation efficiencies of CO-detected galaxies, plotted against their stellar masses. Data points are color-coded in the same manner as the right panel of Figure 1. Adapted from Kokusho et al. (2017).

the PAH luminosities integrating the best-fit PAH model over the wavelength range 5–1000  $\mu\text{m}$ , and then we converted the PAH luminosities to the SFRs with the method proposed by Shipley et al. (2016). The blue, green, and red points in the figure show the ETGs with the mass-weighted stellar population age of 3–7, 7–11, and 11–14 Gyr, respectively (McDermid et al. 2015). The black dotted line represents the correlation between current SFRs and stellar masses of local LTGs (i.e. star formation main sequence; Elbaz et al. 2007). The figure shows that the ETGs possess the current SFRs systematically lower than LTGs, indicating that local ETGs are passive galaxies. The figure also shows that the current SFRs of the ETGs gradually decrease as the stellar age increases, suggesting that ETGs gradually cease to form stars as they evolve.

We estimate the dust masses with the best-fit dust model and the dust mass absorption coefficient described as  $\kappa_\nu \propto \nu^2$ , where we adopted  $\kappa_{140\ \mu\text{m}} = 13.9\ \text{cm}^2\ \text{g}^{-1}$  (Draine 2003). The dust masses and the dust-to-stellar mass ratios of the sample ETGs are estimated to be typically  $10^5$ – $10^7\ M_\odot$  and  $10^{-6}$ – $10^{-4}$ , respectively, which are lower than those of LTGs by two to three orders of magnitude (e.g., Cortese et al. 2012). This result supports that local ETGs are indeed passive galaxies.

#### 4. DISCUSSION

Figure 2 shows the so-called Kennicutt-Schmidt (KS) law, relations between the surface densities of SFRs and gas masses for the sample ETGs. We use the gas masses and source sizes derived in the ATLAS<sup>3D</sup> survey through CO and H I interferometry observations (Alatalo et al. 2013; Young et al. 2014; Davis et al. 2014). Considering that molecular gas plays a crucial role in star formation, we adopted 56 CO-detected ETGs to investigate the KS law. The black dotted line and gray shaded region show the relation of local LTGs and its intrinsic scatter, respectively (Kennicutt 1998). The figure reveals that the sample ETGs follow the relation of LTGs, implying that the current star formation efficiencies (SFEs) of ETGs are similar to those of LTGs. More clearly, Figure 3 shows the current SFEs of CO-detected ETGs, plotted against their stellar masses. The data points are color-coded by the stellar population age of each galaxy. The figure demonstrates that the current SFEs of the ETGs do not depend on either stellar mass or age, suggesting that the current star formation in local ETGs is not suppressed, i.e. the SFEs are not lowered, by merger-induced processes. Hence the low SFRs of ETGs are likely to be caused by their lower amounts of the cold ISM.

We also find that the sample ETGs show the dust-to-gas mass ratios similar to LTGs (Kokusho et al., in prep.). Since the dust-to-gas mass ratio is a proxy of gas-phase metallicities (e.g., Rémy-Ruyer et al. 2013), this result suggests that ETGs are likely to possess metal abundances similar to LTGs. Therefore, although local ETGs show smaller amounts of the cold ISM and lower SFRs than LTGs, ETGs are likely to possess the cold ISM and star formation properties, such as metallicities and SFEs, similar to LTGs.

#### 5. SUMMARY

With the AKARI-all sky maps, we performed a systematic study of the ISM and star formation of the 260 local ETGs from the ATLAS<sup>3D</sup> survey. Modeling SEDs of the sample ETGs, we derive the total dust and PAH luminosities, and thus total dust masses and SFRs. We find that the current SFRs and the dust-to-stellar mass ratios of the ETGs are systematically lower than those of LTGs and that the SFRs gradually decrease as the stellar population age increases, implying that local ETGs gradually cease to form stars. We also find that the current SFEs of the ETGs are similar to those of LTGs, and the SFEs depend on neither stellar mass nor age. Our results suggest that low SFRs of local ETGs are likely caused by their smaller amounts of the cold ISM rather than a suppression of star formation.

**ACKNOWLEDGMENTS**

This research is based on observations with *AKARI*, a JAXA project with the participation of ESA.

**REFERENCES**

- Alatalo, K., Davis, T. A., Bureau, M., et al. 2013, *MNRAS*, 432, 1796  
Amblard, A., Riguccini, L., Temi, P., et al. 2014, *ApJ*, 783, 135  
Cappellari, M., Emsellem, E., Krajnović, D., et al. 2011, *MNRAS*, 413, 813  
Cappellari, M., Scott, N., Alatalo, K., et al. 2013, *MNRAS*, 432, 1709  
Cortese, L., Ciesla, L., Boselli, A., et al. 2012, *A&A*, 540, A52  
de Zeeuw, P. T., Bureau, M., Emsellem, E., et al. 2002, *MNRAS*, 329, 513  
Davis, T. A., Young, L. M., Crocker, A. F., et al. 2014, *MNRAS*, 444, 3427  
Doi, Y., Takita, S., Ootsubo, T., et al. 2015, *PASJ*, 67, 50  
Draine, B. T. 2003, *ARA&A*, 41, 241  
Draine, B. T., & Li, A. 2007, *ApJ*, 657, 810  
Elbaz, D., Daddi, E., Le Borgne, D., et al. 2007, *A&A*, 468, 33  
Hopkins, P. F., Hernquist, L., Cox, T. J., & Kereš, D. 2008, *ApJS*, 175, 356-389  
Kennicutt, R. C., Jr. 1998, *ApJ*, 498, 541  
Kokusho, T., Kaneda, H., Bureau, M., et al. 2017, *A&A*, 605, A74  
McDermid, R. M., Alatalo, K., Blitz, L., et al. 2015, *MNRAS*, 448, 3484  
Rémy-Ruyer, A., Madden, S. C., Galliano, F., et al. 2013, *A&A*, 557, A95  
Schawinski, K., Khochfar, S., Kaviraj, S., et al. 2006, *Nature*, 442, 888  
Serra, P., Oosterloo, T., Morganti, R., et al. 2012, *MNRAS*, 422, 1835  
Shiple, H. V., Papovich, C., Rieke, G. H., Brown, M. J. I., & Moustakas, J. 2016, *ApJ*, 818, 60  
Smith, M. W. L., Gomez, H. L., Eales, S. A., et al. 2012, *ApJ*, 748, 123  
Temi, P., Mathews, W. G., Brighenti, F., & Bregman, J. D. 2003, *ApJL*, 585, L121  
Thomas, D., Maraston, C., Schawinski, K., Sarzi, M., & Silk, J. 2010, *MNRAS*, 404, 1775  
Young, L. M., Bureau, M., Davis, T. A., et al. 2011, *MNRAS*, 414, 940  
Young, L. M., Scott, N., Serra, P., et al. 2014, *MNRAS*, 444, 3408